

Chaos in nanomagnet via feedback current

Tomohiro Taniguchi¹, Nozomi Akashi², Hirofumi Notsu^{3,4},
Masato Kimura³, Hiroshi Tsukahara⁵, and Kohei Nakajima²

¹*National Institute of Advanced Industrial Science and Technology (AIST),
Spintronics Research Center, Tsukuba, Ibaraki 305-8568, Japan,*

²*Graduate School of Information Science and Technology,
The University of Tokyo, Bunkyo-ku, 113-8656 Tokyo, Japan,*

³*Faculty of Mathematics and Physics, Institute of Science and Engineering,
Kanazawa University, Kanazawa, Ishikawa 920-1164, Japan,*

⁴*JST, PRESTO, 4-1-8 Honcho, Kawaguchi, Saitama 332-0012, Japan,*

⁵*High Energy Accelerator Research Organization (KEK), Tsukuba, Ibaraki 305-0801, Japan*
(Dated: September 13, 2019)

Nonlinear magnetization dynamics excited by spin-transfer effect with feedback current is studied both numerically and analytically. The numerical simulation of the Landau-Lifshitz-Gilbert equation indicates the positive Lyapunov exponent for a certain range of the feedback rate, which identifies the existence of chaos in a nanostructured ferromagnet. Transient behavior from chaotic to steady oscillation is also observed in other range of the feedback parameter. An analytical theory is also developed, which indicates the appearance of multiple attractors in a phase space due to the feedback current. An instantaneous imbalance between the spin-transfer torque and damping torque causes a transition between the attractors, and results in the complex dynamics.

PACS numbers:

Nonlinear dynamics can be found in a wide variety of physical, chemical, and biological systems from small to large scale [1,2]. Recent observations of rich magnetization dynamics, such as switching, auto-oscillation (limit cycle), and synchronization, excited in a nanostructured ferromagnet have also proved the applicability of nonlinear science to a fine structure [3–12]. These dynamics are driven by spin current carried by, for example, conducting electrons in metals [13–15]. Since the spin current in metals can survive only within nanometer scale [16], these magnetization dynamics had not been observed until the development of fabrication technology of nanostructure was achieved. A new direction investigating the applicability of such nonlinear magnetization dynamics to new computing scheme, inspired by human brain, has been growing very recently [17–20].

An attractive phenomenon in nonlinear science is chaos [21,22]. Unfortunately, whereas it has been clarified that the magnetization dynamics in a nanostructured ferromagnet is well described by simplified models such as macrospin model or Thiele equation [23–28], the Poincaré-Bendixson theorem prohibits chaos because the models include only two dynamical variables [21]. Thus, an additional degree of freedom is necessary to induce chaos in ferromagnets. In previous works, chaos has been studied for systems with alternative current [29,30] or magnetic and/or electric interaction between two ferromagnets [31,32]. Another possible source causing highly nonlinear dynamics is feedback force with delay [33]. Recently, the modulation of the threshold current by the self-injection of the feedback current into the vortex ferromagnet was predicted theoretically [34] and was experimentally confirmed [35]. Complex dynamics in an in-plane magnetized ferromagnet with feedback current was also found by numerical simulation [36]. However,

the existence of the feedback effect does not necessarily guarantee chaos. Therefore, a careful analysis of the magnetization dynamics in the presence of feedback effect is necessary to identify chaos.

The purpose of this work is to develop a theoretical analysis of the nonlinear magnetization dynamics in a nanostructured ferromagnet in the presence of feedback current. We perform the numerical simulation of the Landau-Lifshitz-Gilbert (LLG) equation in spin torque oscillator (STO), and find that the feedback current causes highly nonlinear dynamics of the magnetization. The present work identifies chaos by the positive Lyapunov exponent, which is found in a certain range of the feedback rate, whereas transient behavior is also observed in other range of the feedback rate. We also develop an analytical theory to reveal the origin of such complex dynamics. The bifurcation analysis indicates that the feedback current results in the appearance of multiple attractors in the phase space. An instantaneous imbalance between the spin-transfer torque and damping torque allows a transition between these attractors, and induces the complex dynamics found in the numerical analysis.

The system under consideration is schematically shown in Fig. 1(a). The unit vectors pointing in the magnetization directions in free and reference layers are denoted as \mathbf{m} and \mathbf{p} , respectively. Direct current, I , is injected from the reference to free layer, and excites an auto-oscillation of the magnetization \mathbf{m} via spin-transfer effect [13,14]. Here, we focus on the STO consisting of a perpendicularly magnetized free layer and an in-plane magnetized reference layer because this type of STO can emit large emission power with narrow linewidth [10], and therefore, is of great interest from viewpoints of both fundamental and applied physics. The magnetization \mathbf{p} in the reference layer points to the positive x direction, whereas the

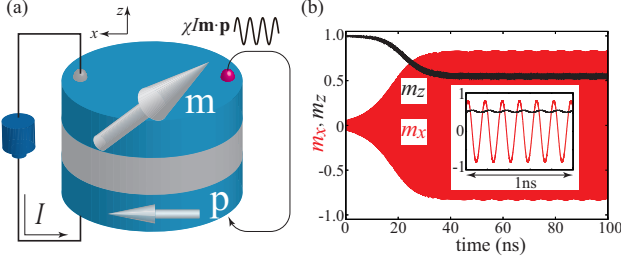


FIG. 1: (a) Schematic view of the system. The direct current I is injected from the reference layer to the positive layer, whereas the current, $\chi I \mathbf{m} \cdot \mathbf{p}$, outputted from the STO is injected into the STO with time delay τ . The feedback current oscillates when the magnetization \mathbf{m} in the free layer is in a dynamical state. (b) Typical magnetization dynamics in the absence of the feedback current. The inset shows an auto-oscillation in a steady state.

z axis is perpendicular to the film-plane. The magnetization dynamics in the free layer is described by the Landau-Lifshitz-Gilbert (LLG) equation given by

$$\frac{d\mathbf{m}}{dt} = -\gamma \mathbf{m} \times \mathbf{H} - \gamma H_s \mathbf{m} \times (\mathbf{p} \times \mathbf{m}) + \alpha \mathbf{m} \times \frac{d\mathbf{m}}{dt} \quad (1)$$

where γ and α are the gyromagnetic ratio and the Gilbert damping constant respectively. The magnetic field $\mathbf{H} = [H_{\text{appl}} + (H_K - 4\pi M)m_z]\mathbf{e}_z$ consists of an applied field H_{appl} , interfacial magnetic anisotropy field H_K [37–39], and demagnetization field $-4\pi M$. The spin-transfer torque strength, H_s is given by

$$H_s = \frac{\hbar \eta I [1 + \chi \mathbf{m}(t - \tau) \cdot \mathbf{p}]}{2e(1 + \lambda \mathbf{m} \cdot \mathbf{p})MV}, \quad (2)$$

where M and V are the saturation magnetization and the volume of the free layer, respectively. The spin-transfer torque strength is characterized by the spin polarization η and spin-transfer torque asymmetry λ . The values of the parameters used in this work are derived from the experiment [10], as well as a theoretical analysis [40]; see Supplemental Material [41]. Figure 1(b) shows a typical magnetization dynamics in the absence of the feedback current, where the direct current is $I = 2.5$ mA. As shown, an auto-oscillation having a period of 0.16 ns is excited after a relaxation time on the order of 10 ns. The inset of Fig. 1(b) shows the dynamics of m_x (red) and m_z (black) in a steady state. It can be seen from the figure that m_z is almost temporally constant but slightly oscillates around a certain value. These results will be used for comparison with the dynamics in the presence of the feedback current, as well as for the development of an analytical theory, below.

The strength of the spin-transfer torque, Eq. (2), includes the feedback current given by $\chi I \mathbf{m}(t - \tau) \cdot \mathbf{p}$, where χ is the rate of the feedback current with respect to the direct current I , whereas τ is the delay time. Due to tunnel magnetoresistance effect, the feedback current depends on the relative direction of the magnetizations,

$\mathbf{m} \cdot \mathbf{p}$ [10]. The feedback current brings the past information of the magnetization state, and extends the dimension of the phase space, which presents a possibility to excite chaos in STO. Note that the feedback current can be injected to the STO independently from the direct current by using a bias-Tee and delay line, where the typical value of the delay time possible in experiment is on the order of 1 – 10 ns [35].

The LLG equation, Eq. (1), with the feedback current is solved by a fourth-order Runge-Kutta scheme accompanied with continuation method (see Supplemental Material [41] in detail). Figures 2(a)-2(c) show the time evolutions of $m_z(t)$ for $\chi = 0.02$, $\chi = 0.50$, and $\chi = 0.89$, respectively. Note that the time range of each figure is different to understand the characteristics of each dynamics. In the presence of a small feedback current shown in Fig. 2(a), although the amplitude of the oscillation is modulated, the dynamics in the steady state is still periodic. On the other hand, when the feedback rate becomes relatively large, chaotic behavior appears, as shown in Fig. 2(b). In this case, non-periodic and highly nonlinear dynamics appears over a wide time range. The value of m_z oscillates almost over its possible value, $|m_z| \leq 1$. A further increase of the feedback rate leads to a transition of the magnetization dynamics from chaotic to non-chaotic, as shown in Fig. 2(c). The chaotic dynamics suddenly disappears after comparatively long period, i.e., longer than the oscillation period of the limit cycle in the absence of the feedback current. As mentioned below, the Lyapunov exponents of the dynamics in Figs. 2(a) and 2(c) are zero, whereas it is positive for the dynamics in Fig. 2(b).

In the present work, chaos is defined as the dynamics with the positive Lyapunov exponent. The details of the evaluation method of the Lyapunov exponent developed in this work are summarized Supplemental Material [41]. We also evaluate the bifurcation diagram, which is defined as the local maximum of $m_z(t)$ after the magnetization moves to an attractor (the bifurcation diagram of other component, m_x , is shown in Supplemental Material [41]). Figures 3(a) and 3(b) shows the Lyapunov exponent and the bifurcation diagram as a function of the feedback rate in a small range $\chi \leq 0.10$. The Lyapunov exponent remains zero for $\chi \lesssim 0.024$, where the dynamics is a limit cycle, such as shown in Fig. 1(b), or the oscillation with an amplitude modulation as shown in Fig. 2(a). In the limit cycle state, the local maximum of m_z is a single value, whereas it takes several values and shows symmetric distributions around its center in the modulated dynamics, as can be seen in Fig. 3(b). The Lyapunov exponent becomes positive for $\chi \gtrsim 0.025$, where the bifurcation diagram shows an inhomogeneous (asymmetric) structure. The Lyapunov exponent and the bifurcation diagram for a wide range of the feedback rate, $\chi \leq 1.00$, are shown in Figs. 3(c) and 3(d), respectively. The positive Lyapunov exponent indicates the existence of chaos in STO. The Lyapunov exponent becomes zero again when the feedback rate is further

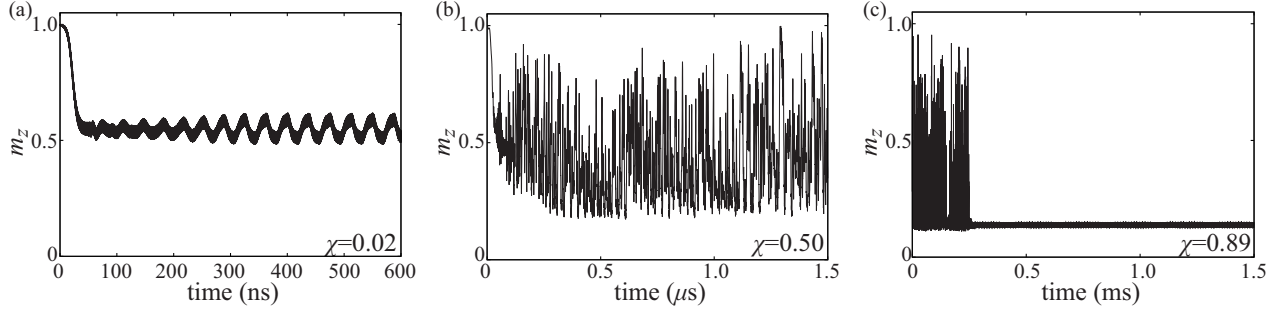


FIG. 2: Time evolutions of $m_z(t)$ for the feedback rates of (a) $\chi = 0.02$, (b) 0.50, and (c) 0.89. The current and the delay time are $I = 2.5$ mA and $\tau = 30$ ns. Note that the time range of each figure is different.

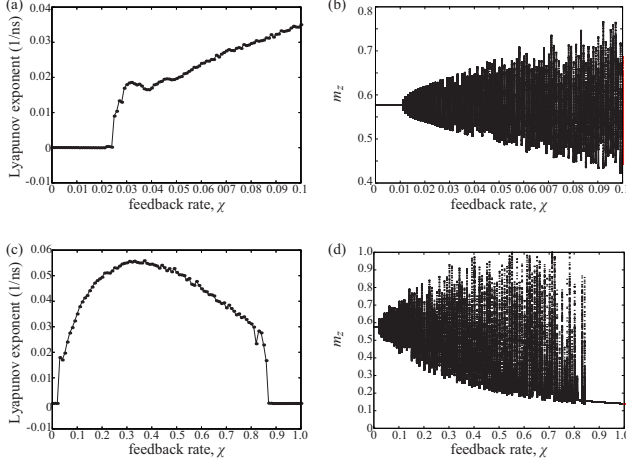


FIG. 3: (a) (maximum) Lyapunov exponent and (b) bifurcation cascade (local maximum of m_z) as a function of the feedback rate $\chi \leq 0.10$. The current and delay time are $I = 2.5$ mA and $\tau = 30$ ns, respectively. The range of χ is extended to $\chi \leq 1.00$ in (c) and (d).

increased to $\chi \simeq 0.087$. The magnetization dynamics shown in Fig. 2(c), corresponding to this parameter region, can be regarded as transient chaos, which can be found in, for example, a spatially extended turbulence model [42], where the dynamical system finally arrives at an attractor with zero or negative Lyapunov exponent long time after showing chaotic behavior [21]. For example, the transient time observed in Fig. 2(c) is on the order of 0.1 ms, which is sufficiently longer than the period of the auto-oscillation in the absence of the feedback current (0.16 ns) but is measurable because it is shorter than the experimentally available time range for STO dynamics reported up to date, 1.6 ms [43]. We should also note that the magnetization dynamics, its bifurcation diagram, and Lyapunov exponent as a function of the delay time are summarized in Supplemental Material [41].

The above numerical results indicate the existence of rich variety of nonlinear dynamics, including chaos, in an STO. Although it is difficult to solve the LLG equation exactly due to its nonlinearity, let us investigate the physical origin of the complex dynamics with help of an approximated theory, which has been known to be useful

to analyze nonlinear dynamics such as auto-oscillation (limit cycle) [28,40] and synchronization [44,45]. An auto-oscillation in an STO is excited when the spin-transfer torque balances with the damping torque, and the field torque, $-\gamma \mathbf{m} \times \mathbf{H}$, remains finite. The field torque leads to a sustainable oscillation of the magnetization on a constant energy curve of the magnetic energy density defined as $E = -M \int d\mathbf{m} \cdot \mathbf{H}$. In the present system, the constant energy curve corresponds to the trajectory with a constant zenith angle $\theta = \cos^{-1} m_z$, where the oscillation frequency, $f(\theta)$, on the constant energy curve is $f(\theta) = \gamma[H_{\text{appl}} + (H_K - 4\pi M) \cos \theta]/(2\pi)$. It should be, however, emphasized that there is often an instantaneous imbalance between the spin-transfer torque and damping torque because of their different angular dependences. Therefore, strictly speaking, θ (or m_z) in the present system is not a constant variable [40]; see also the inset of Fig. 1(b). However, for a sufficiently small damping constant α , the real trajectory of the auto-oscillation is practically close to a constant energy curve. In such a case, it is useful to derive the equation of motion of θ averaged over the precession period $T(\theta) = 1/f(\theta)$ as $\overline{d\theta/dt} \equiv (1/T) \oint dt(d\theta/dt)$, (see Supplemental Material [41] for derivation)

$$\begin{aligned} \frac{\overline{d\theta}}{dt} = & -\alpha\gamma[H_{\text{appl}} + (H_K - 4\pi M) \cos \theta] \sin \theta \\ & + \frac{\gamma H_{s0}}{\lambda \tan \theta} \left(\frac{1}{\sqrt{1 - \lambda^2 \sin^2 \theta}} - 1 \right) p(\chi, \tau, \theta), \end{aligned} \quad (3)$$

where $H_{s0} = \hbar\eta I/(2eMV)$, whereas $p(\chi, \tau, \theta)$ is given by

$$p(\chi, \tau, \theta) = 1 - \frac{\chi}{\lambda} \cos 2\pi f(\theta)\tau. \quad (4)$$

The angle θ satisfying $\overline{d\theta/dt} = 0$ and $d(\overline{d\theta/dt})/d\theta < (>)0$ corresponds to a stable (unstable) fixed point in the reduced phase space [1]. In the absence of feedback current, there is only one stable fixed point (attractor), corresponding to auto-oscillation state in real space, in the present STO [40]. On the other hand, Fig. 4(a) shows an example of $\overline{d\theta/dt}$ in the presence of the feedback. As shown, several attractors satisfying $\overline{d\theta/dt} = 0$ and $d(\overline{d\theta/dt})/d\theta < 0$ appear due to the feedback current.

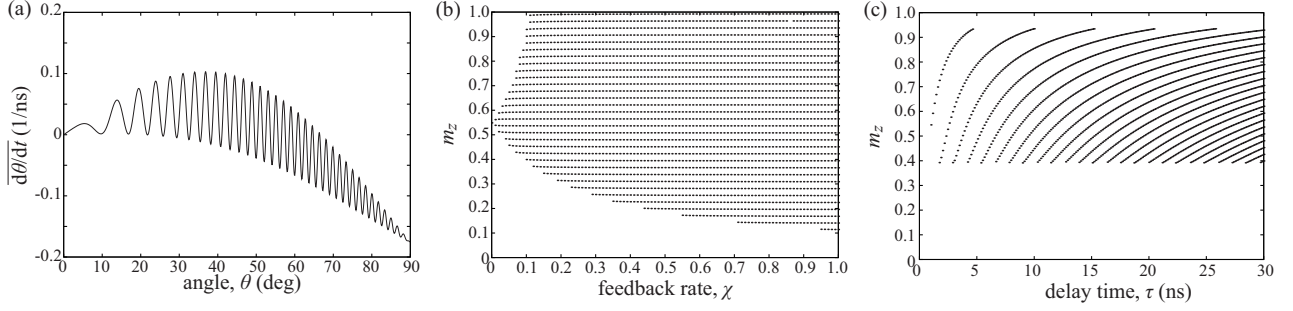


FIG. 4: (a) The averaged $d\theta/dt$ given by Eq. (3) solved in the phase space as a function of $\theta = \cos^{-1} m_z$. The current, feedback rate, and delay time are $I = 2.5$ mA, $\chi = 0.10$, and $\tau = 30$ ns. (b), (c) Stable fixed points $m_z = \cos \theta$ estimated analytically as a function of (b) the feedback rate χ with $\tau = 30$ ns and (c) the delay time τ with $\chi = 0.10$.

Figures 4(b) and 4(c) show the attractors $m_z = \cos \theta$ as a function of the feedback rate χ and the delay time τ , respectively. It can be understood from these figures that the number of the attractor increases with increasing the feedback rate and/or delay time. Let us here call such structure as multiple attractors. Although these results are obtained with an approximation mentioned above, they are useful to understand the origin of the complex magnetization dynamics found by numerical simulation, as discussed below.

The multiple attractors originate from the function $p(\chi, \tau, \theta)$ given by Eq. (4). In the absence of the feedback current ($\chi = 0$), the function $p(\chi, \tau, \theta) = 1$ is independent of the angle θ . On the other hand, in the presence of the feedback current ($\chi \neq 0$), several values of the angle θ give an identical value of $p(\chi, \tau, \theta)$ because the function includes a periodic (cosine) function depending on θ . As a result, several θ can simultaneously satisfy the conditions of the stable fixed point.

The origin of the complex dynamics found in the numerical simulation is considered to be the existence of multiple attractors. Since the attractors locate discretely, as shown in Fig. 4, one might consider that once the magnetization is trapped by one of the attractors, it cannot move to the others. It should be, however, reminded that the assumption of a constant angle θ was used in the derivation of Eq. (3). As emphasized above, the real angle $\theta = \cos^{-1} m_z$ in a limit cycle slightly oscillates around the fixed point estimated analytically by Eq. (3) because of the instantaneous imbalance between the spin-transfer torque and damping torque. As a result, the magnetization can move from one attractor to the other when the distance between the attractors is smaller than the oscillation amplitude of the angle θ . The transition between the attractors causes the highly complex dynamics shown in Fig. 2, contrary to the system without feedback in which an auto-oscillation state is uniquely determined.

It is considered that the above analytical theory can be applied to any type of STO, although Eq. (3) was derived for its specific type. For example, the complex dynamics found in an in-plane magnetized STO [36] maybe caused

by the same mechanism, i.e., the appearance of multiple attractors due to the existence of feedback current. The periodicity of the multiple attractors in this type of STO is described by elliptic functions in contrast with Eq. (4) where the periodicity is described by a simple trigonometric function; see Supplemental Material in detail [41].

In conclusion, the nonlinear magnetization dynamics in a spin torque oscillator was studied by taking into account the effect of spin-transfer torque excited by the feedback current. The numerical simulation reveals rich variety of the nonlinear magnetization dynamics, which can be controlled by the feedback parameter. The positive Lyapunov exponent for a certain range of the feedback rate indicated the existence of chaos in the spin torque oscillator, whereas transient behavior from chaotic to steady state was also observed in other range of the feedback parameter. The analytical theory based on the averaged equation of motion revealed that the feedback current results in the multiple attractors in the phase space. The number of the attractors increased with increasing the feedback rate and/or delay time. An instantaneous imbalance between the spin-transfer torque and damping torque caused a transition between the attractors, and induces the complex magnetization dynamics.

The authors are thankful to Joo-Von Kim, Takehiko Yorozu, Sumito Tsunegi, and Shinji Miwa for valuable discussion. T. T. is grateful to Satoshi Iba, Aurelie Spiesser, Hiroki Maehara, and Ai Emura for their support and encouragement. The results were partially obtained from a project (Innovative AI Chips and Next-Generation Computing Technology Development/(2) Development of next-generation computing technologies/Exploration of Neuromorphic Dynamics towards Future Symbiotic Society) commissioned by NEDO. K. N. is supported by JSPS KAKENHI Grant Numbers JP18H05472, and JP16KT0019. H. N. is supported by JSPS KAKENHI Grant Number JP18H01135, and JST PRESTO Grant Number JPMJPR16EA. M. K. is supported by JSPS KAKENHI Grant Numbers JP16H02155, JP17H02857.

- ¹ S. H. Strogatz, *Nonlinear Dynamics and Chaos: With Applications to Physics, Biology, Chemistry, and Engineering* (Westview Press, 2001), 1st ed.
- ² A. Pikovsky, M. Rosenblum, and J. Kurths, *Synchronization: A universal concept in nonlinear sciences* (Cambridge University Press, 2003), 1st ed.
- ³ J. A. Katine, F. J. Albert, R. A. Buhrman, E. B. Myers, and D. C. Ralph, Phys. Rev. Lett. **84**, 3149 (2000).
- ⁴ S. I. Kiselev, J. C. Sankey, I. N. Krivorotov, N. C. Emley, R. J. Schoelkopf, R. A. Buhrman, and D. C. Ralph, Nature **425**, 380 (2003).
- ⁵ W. H. Rippard, M. R. Pufall, S. Kaka, S. E. Russek, and T. J. Silva, Phys. Rev. Lett. **92**, 027201 (2004).
- ⁶ G. Bertotti, C. Serpico, I. D. Mayergoyz, A. Magni, M. d'Aquino, and R. Bonin, Phys. Rev. Lett. **94**, 127206 (2005).
- ⁷ A. Slavin and V. Tiberkevich, Phys. Rev. Lett. **95**, 237201 (2005).
- ⁸ D. Houssameddine, U. Ebels, B. Delaët, B. Rodmacq, I. Firastrau, F. Ponthenier, M. Brunet, C. Thirion, J.-P. Michel, L. Prejbeanu-Buda, et al., Nat. Mater. **6**, 447 (2007).
- ⁹ J.-V. Kim, V. Tiberkevich, and A. N. Slavin, Phys. Rev. Lett. **100**, 017207 (2008).
- ¹⁰ H. Kubota, K. Yakushiji, A. Fukushima, S. Tamaru, M. Konoto, T. Nozaki, S. Ishibashi, T. Saruya, S. Yuasa, T. Taniguchi, et al., Appl. Phys. Express **6**, 103003 (2013).
- ¹¹ E. Grimaldi, A. Dussaux, P. Bortolotti, J. Grollier, G. Pillet, A. Fukushima, H. Kubota, K. Yakushiji, S. Yuasa, and V. Cros, Phys. Rev. B **89**, 104404 (2014).
- ¹² A. A. Awad, P. Dürrenfeld, A. Houshang, M. Dvornik, E. Iacoca, R. K. Dumas, and J. Akerman, Nat. Phys. **13**, 292 (2017).
- ¹³ J. C. Slonczewski, J. Magn. Magn. Mater. **159**, L1 (1996).
- ¹⁴ L. Berger, Phys. Rev. B **54**, 9353 (1996).
- ¹⁵ D. C. Ralph and M. D. Stiles, J. Magn. Magn. Mater. **320**, 1190 (2008).
- ¹⁶ T. Valet and A. Fert, Phys. Rev. B **48**, 7099 (1993).
- ¹⁷ J. Grollier, D. Querlioz, and M. D. Stiles, Proc. IEEE **104**, 2024 (2016).
- ¹⁸ J. Torrejon, M. Riou, F. A. Araujo, S. Tsunegi, G. Khalsa, D. Querlioz, P. Bortolotti, V. Cros, K. Yakushiji, A. Fukushima, et al., Nature **547**, 428 (2017).
- ¹⁹ K. Kudo and T. Morie, Appl. Phys. Express **10**, 043001 (2017).
- ²⁰ T. Furuta, K. Fujii, K. Nakajima, S. Tsunegi, H. Kubota, Y. Suzuki, and S. Miwa, Phys. Rev. Applied **10**, 034063 (2018).
- ²¹ K. T. Alligood, T. D. Sauer, and J. A. Yorke, *Chaos. An Introduction to Dynamical Systems* (Springer (New York), 1997).
- ²² E. Ott, *Chaos in Dynamical Systems* (Cambridge University Press (Cambridge), 2002), 2nd ed.
- ²³ J. Z. Sun, Phys. Rev. B **62**, 570 (2000).
- ²⁴ J. Grollier, V. Cros, H. Jaffrès, A. Hamzic, J. M. George, G. Faini, J. B. Youssef, H. L. Gall, and A. Fert, Phys. Rev. B **67**, 174402 (2003).
- ²⁵ G. Tatara and H. Kohno, Phys. Rev. Lett. **92**, 086601 (2004).
- ²⁶ K. Y. Guslienko, X. F. Han, D. J. Keavney, R. Divan, and S. D. Bader, Phys. Rev. Lett. **96**, 067205 (2006).
- ²⁷ A. Slavin and V. Tiberkevich, IEEE. Trans. Magn. **45**, 1875 (2009).
- ²⁸ G. Bertotti, I. Mayergoyz, and C. Serpico, *Nonlinear magnetization Dynamics in Nanosystems* (Elsevier, Oxford, 2009).
- ²⁹ Z. Li, C. Li, and S. Zhang, Phys. Rev. B **74**, 054417 (2006).
- ³⁰ Z. Yang, S. Zhang, and Y. C. Li, Phys. Rev. Lett. **99**, 131401 (2007).
- ³¹ K. Kudo, R. Sato, and K. Mizushima, Jpn. J. Appl. Phys. **45**, 3869 (2006).
- ³² T. Taniguchi, J. Magn. Magn. Mater. **483**, 281 (2019).
- ³³ M. C. Mackey and L. Glass, Science **197**, 287 (1977).
- ³⁴ G. Khalsa, M. D. Stiles, and J. Grollier, Appl. Phys. Lett. **106**, 242402 (2015).
- ³⁵ S. Tsunegi, E. Grimaldi, R. Lebrun, H. Kubota, A. S. Jenkins, K. Yakushiji, A. Fukushima, P. Bortolotti, J. Grollier, S. Yuasa, et al., Sci. Rep. **6**, 26849 (2016).
- ³⁶ J. Williams, A. D. Accioly, D. Rontani, M. Sciamanna, and J.-V. Kim, Appl. Phys. Lett. **114**, 232405 (2019).
- ³⁷ S. Yakata, H. Kubota, Y. Suzuki, K. Yakushiji, A. Fukushima, S. Yuasa, and K. Ando, J. Appl. Phys. **105**, 07D131 (2009).
- ³⁸ S. Ikeda, K. Miura, H. Yamamoto, K. Mizunuma, H. D. Gan, M. Endo, S. Kanai, J. Hayakawa, F. Matsukura, and H. Ohno, Nat. Mater. **9**, 721 (2010).
- ³⁹ H. Kubota, S. Ishibashi, T. Saruya, T. Nozaki, A. Fukushima, K. Yakushiji, K. Ando, Y. Suzuki, and S. Yuasa, J. Appl. Phys. **111**, 07C723 (2012).
- ⁴⁰ T. Taniguchi, T. Ito, S. Tsunegi, H. Kubota, and Y. Utsumi, Phys. Rev. B **96**, 024406 (2017).
- ⁴¹ Supplemental Material.
- ⁴² J. P. Crutchfield and K. Kaneko, Phys. Rev. Lett. **60**, 2715 (1988).
- ⁴³ S. Tsunegi, T. Taniguchi, R. Lebrun, K. Yakushiji, V. Cros, J. Grollier, A. Fukushima, S. Yuasa, and H. Kubota, Sci. Rep. **8**, 13475 (2018).
- ⁴⁴ T. Taniguchi, Phys. Rev. B **95**, 104426 (2017).
- ⁴⁵ T. Taniguchi, Phys. Rev. B **98**, 104417 (2019).